Surface Hardness and Abrasion Threshold of Chemically Strengthened Soda-Lime Silicate Glasses After Steam Processing

Gohar Sani[1], Roman Sajzew[1] iD, Rene Limbach[1] iD, Shigeki Sawamura[2], Akio Koike[2] and Lothar Wondraczek[1] iD

[1] Otto Schott Institute of Materials Research, Friedrich Schiller University Jena, Jena, Germany

[2] Materials Integration Laboratories, AGC Inc, Kanagawa, Japan

Abstract. Chemical strengthening by diffusive ion exchange (IOX) is a common method to improve the mechanical performance of glass products. However, the process of ion-stuffing is often associated with an increase of surface hardness and a decrease of the resistance to abrasive wear during scratching, even when the thickness of the exchanged layer is low. Autoclave steam-treatment presents a way to compensate the enhanced surface brittleness accompanying IOX. It causes a notable shift in the load threshold for microabrasion to more abrasion-resistant glasses. Subject to the specific processing parameters, the softening effect is constrained to a surface layer of less than 500 nm in thickness; therefore, the overall compressive stress profile is not affected and the advantages of IOX strengthening are retained. In turn, ion-stuffing by IOX counteracts severe autoclave corrosion of soda-lime silicate glasses, making them suitable for a combination of both processes.

Keywords: Chemical strengthening, Mechanical properties, Steam, Defect resistance, Abrasive wear

1. Introduction

Silicate glasses are ubiquitous in architecture [1], packaging [2], electronics [3], telecommunication [4] and transport [5]. In many of these applications, glass products are exposed to harsh environments [6] and abrasive wear [7], [8]. Surface flaws and defects generated from such exposure reduce the mechanical performance of a glass product by orders of magnitude [9]. While variations in chemical composition can be adapted in order to enhance the defect resistance of glasses [10], [11], the range of glass formulations suitable for practical application has remained limited by constraints in production cost, volume needs and processing capability. Post-processing techniques have therefore been established by which the mechanical properties of glass surfaces can be improved [12]. Most prominently, thermal or chemical strengthening are widely employed to impose a surface compressive layer which counteracts tensile loading [9]. Thermal strengthening requires relatively thick glass sheet (or container walls) and rapid quenching of the surface of a hot glass product [13], for example to be used as solar covers, safety windows or in roof-top applications. Chemically strengthened glasses are produced by diffusive exchange of the mobile alkali ions (IOX) present in the precursor glass through immersion of the glass in a bath of molten salt. Thereby, IOX of smaller alkali species (Li^+ or Na^+) by larger ones (typically K^+) at a temperature below the glass transition T_g creates a surface compressive layer [14], [15]. Regarding the length scale of diffusive exchange, chemical strengthening is suitable for thin glass products; it is commonly applied for display covers and bendable or flexible glass sheets [16], but has also been used in other

applications such as pharmaceutical packaging [17], or smart window devices [18]. For benchmark aluminosilicate glasses, the surface compressive stress (CS) generated by IOX reaches a level of ~ 1 GPa. As the second target parameter affecting surface defect resistance, the depth of the IOX layer (DOL) is typically on the order of 10^2 µm, but may be also as low as 10 µm. Both parameters depend on base glass chemistry, IOX bath composition and processing details; they are usually much lower for the commodity soda lime silicate (SLS) glass [19]–[21]. As a downside, the higher atomic packing density resulting from ion stuffing by IOX reduces the threshold load for scratch-induced microcracking and abrasion [21].

Given its commercial relevance, a substantial amount of work has been devoted to the understanding of the IOX process, *e.g.*, regarding the structural origin of the compressive stress layer [22]–[26] or resulting optical and mechanical properties [7], [14], [27], [28]. Aside further tailoring surface mechanical performance, a major objective is to find possible routes which could enable faster IOX at lower temperature, thus improving throughput and processing cost for wider applicability. For example, it was shown that H_2O vapor treatments can be used to modify the surface mechanics of various silicate glasses in very short treatment times[29]. Similar to IOX, the incorporation of water into the glass surface is thought to enable the generation of persistent layers of compressive stress [30], [31], while also affecting material plasticity, elastic properties and fracture characteristics [32], [33].

Here, we combine IOX with subsequent steam treatment at elevated temperatures on commodity soda-lime silicate glass in order to impose chemically strengthened glasses with additional resistance to scratch and abrasion damage. Statistical data are provided on how such combined treatments induce variations in the threshold loads for microcracking and abrasive wear at silicate glass surfaces.

2. Materials and methods

2.1 Chemical strengthening

A commercial soda-lime silicate (SLS) float glass was used as the base material in this study (Sisecam, Turkey). All surface-specific analyses were performed on the air-side of the glass. Pristine sheets of glass with a thickness of 1.10 mm were cleaned in two 5 min cycles of ultrasonication, first immersed in de-ionized (DI) water and subsequently in ethanol. Cleaned samples were dried with compressed air before being immersed into a molten KNO_3 salt bath to induce Na^+/K^+ ion-exchange. Two conditions were chosen for IOX, *i.e.*, a more "typical" exchange temperature of ~0.85 T_g (420 °C) and a more extreme condition at ~0.9 T_g (470 °C); the latter would potentially allow for a certain degree of structural relaxation in parallel to IOX over the exchange time of 8 h. Values of CS and DOL were evaluated using a surface stress meter (FSM-6000LE, Luceo Co., Ltd.) by averaging over two measurements on the same position perpendicular to each other. IOX conditions and resulting CS and DOL parameters are summarized in Table 1.

Table 1. *Ion-exchange (IOX) conditions and resulting surface compressive stress (CS) and depth-of-layer (DOL) in untreated and steam treated (labelled "ST") chemically strengthened soda-lime silicate glasses. IOX treatment times were 8 h for all samples. The instrument accuracy is ± 20 MPa for CS and ± 2 µm for DOL [34].*

Sample Code	IOX treatment temperature (°C)	CS (MPa)	DOL (µm)
SLS	*pristine base glass*	-	-
IOX420	420	723	6.8
IOX420-ST	420	707	6.8
IOX470	470	483	22.7
IOX470-ST	470	479	22.6

2.2 Steam treatment

Steam treatment was conducted in a laboratory high-pressure reactor (Novoclave 600, Büchi AG, Switzerland) that was filled to 20% capacity with DI water. Glass samples (~10 x 20 mm²) were placed vertically above the liquid water level on a stainless-steel holder to ensure exposure to avoid immersion in liquid water. Treatments in saturated steam lasted for 24 h at T=150 °C ± 5 °C (~5 bar). Samples were recovered after cooling the reactor to a temperature below 80 °C within 30 min. For reference, ambient-pressure steam corrosion experiments were conducted in a climate control chamber (VCL 4003, Vötsch) at 80 °C and 80 % relative humidity (r.H.) for 1030 h. The purpose of creating these reference samples was to elucidate the difference between (intentional, high-pressure) autoclave treatment and (unintentional) long-term corrosion at ambient pressure. Aside such comparison, the latter is not in the scope of this study.

2.3 Characterization

Spectroscopy

Potential reaction of the glass with water was analyzed by Fourier-transform infrared spectroscopy (FT-IR) in transmittance (Perkin Elmer Spotlight 200i). An average of 10 spectra was recorded in the range of 7800 to 400 cm^{-1} at a resolution of 2 cm^{-1}. Three measurements were carried out on each sample at different locations. The presented data are averages of these three measurements. UV-Vis transmission and reflection spectra were collected using a double-beam spectrometer (Cary 5000, Agilent Technologies) under 6° incidence, over the wavelength range of 250 to 800 nm, with a slit size of 1 nm and a scan rate of 30 nm min^{-1}.

Grazing Incidence X-ray diffraction

Grazing Incidence X-ray diffraction (GID) was employed in order to identify any surface crystallization reactions following steam treatment and corrosion, respectively. For this purpose, an X-ray diffractometer (Rigaku Smartlab) was used with a 3 kW Cu-K$_\alpha$ X-ray generator, 5° Soller slits and a 0.5° parallel-slit analyzer to complement the parallel-beam configuration. Diffraction patterns were collected for the 2θ range of 10 to 60° at a scan rate of 2.5 °/min with a fixed incidence angle of 1°.

Surface topography

Surface microstructure was investigated on samples without any conductive coating using a low-vacuum scanning electron microscope (JEOL 6510LV) at 20 kV acceleration in electron backscattering mode. Surface roughness was characterized with optical profilometry using a confocal laser scanning microscope (Zeiss Axio LSM700) with a 488 nm laser and a 50x objective (NA0.8). Measurements were performed at three different positions on the same sample for each treatment condition. Surface roughness (root mean square value) was determined on areas of 20 x 20 μm^2 according to ISO 25178. The surface roughness values obtained in this way were used as qualitative measures. Due to the physical limitations of determining roughness on transparent materials with an optical method [35], they are denoted *effective roughness*.

Indentation and scratch behavior

Characterization of the surface mechanical properties was carried out by instrumented nano-indentation (G200, KLA Co.) with a Berkovich diamond tip (Synton-MDP Inc.) using the continuous stiffness measurement (CSM) mode similar to previous studies [21], [36], [37]. Depth profiles of surface Young's modulus E and hardness H were recorded over a displacement range of 2 μm from a total amount of 20 indentations per sample, created at constant strain-rate of 0.05 s^{-1}. Constant-load scratching experiments were carried out with another Berkovich

indentation stylus in edge-forward orientation, monitoring the lateral force acting on the tip upon plowing through the glass at a constant scratch velocity of 50 µm s^{-1}. On each glass sample, sets of 10 tests were performed at different normal loads from 30 to 150 mN over a scratch length L_s = 200 µm. The work of deformation (W_s) and the scratching volume (V_s), which in turn provide the scratch hardness H_s, were calculated according to [38]. Ramp-load scratch testing was carried out using a sphero-conical stylus (Synton- MDP Inc.) having a nominal tip radius of 5.10 µm and a 60° cone opening angle. On each glass sample, 25 scratches were created with a monotonically increasing load up to 325 mN over a scratch length of 650 µm, at a scratch velocity of 50 µm s^{-1} [21], [37], Post-mortem images of scratch grooves obtained in this way were taken on a wide-field confocal microscope (Zeiss Smartproof 5).

3. Results and discussions

IOX and steam treatment

Surface stress profiles obtained after chemical strengthening and after steam treatment are presented in Figure 1A, showing the strong impact of the exchange temperature on CS and DOL [39]. Steam treatment does not seem to notably affect the profiles. No crystallization was detected by GID on any of the samples following steam treatment (Fig. 1B). Variations in the shape and position of the amorphous hump detected by GID cannot be interpreted unambiguously at this stage, given the variations in ion stuffing, water interaction and structural relaxation. The FTIR transmittance data (Fig. 1C) indicate the presence of molecular water ($H_2O^{(m)}$, ~1.9 µm) after steam treatment, in particular, for IOX470-ST. The strength of the H_2O-related absorption bands is a qualitative indicator for the extent of water uptake, which is depending on the way each glass was processed before steam treatment. Sample IOX470-ST exhibiting the strongest water uptake provides confirmation that reduced stuffing (by partial structural relaxation at elevated temperature) favors the incorporation of water [32], [40]–[42]. In addition, the potassium-containing glass (after IOX) is more sensitive to steam treatment than the pristine SLS surface [30], [43]. This underpins the importance of initial IOX conditions for tailoring the effects of subsequent steam treatment. As ion-exchange is rarely performed at 0.9 T_g, (here: ~470 °C) the sample exchanged at 470 °C does not represent a typical IOX glass and will be omitted from our further discussion.
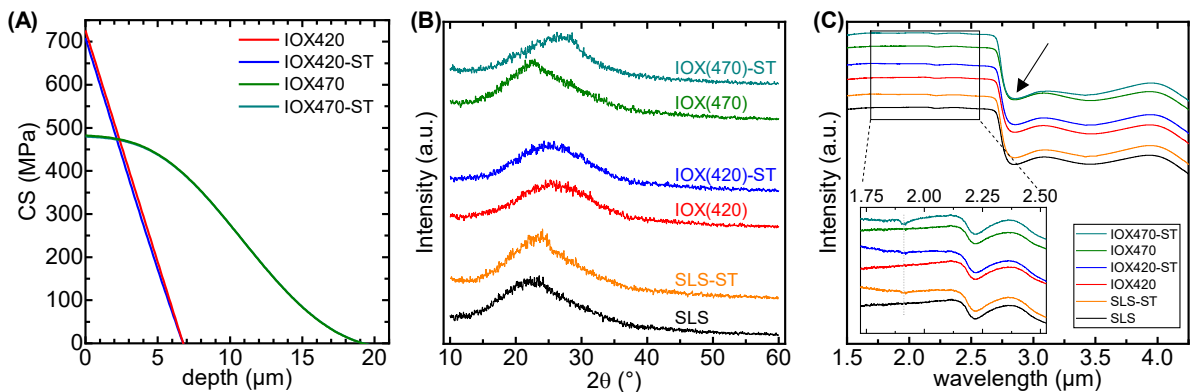
Figure 1. *(A) Stress profiles of IOX glasses before and after steam treatment ("ST"; profiles are strongly overlapping). Values of CS and DOL are provided in Table 1. (B) Grazing Incidence X-ray diffraction patterns of the pristine SLS and ion-exchanged glass surfaces before and after steam treatment. (C) FTIR transmittance spectra. Absorption bands related to molecular water and total water are marked at ~1.9 µm and ~2.9 µm, respectively.*

Microscopic changes of the glass surfaces upon steam treatment are shown in Figure 2. In particular, the corroded SLS sample SLS-ST-CC exhibited a significant loss in direct light transmission caused by optical scattering, whereas changes on all other glasses were much less

pronounced (Fig. 2A). The origin of optical scattering is revealed in the correlation between effective surface roughness and average scattered intensity (Fig. 2B; the average scattered intensity S is estimated for the visible spectral range of 400-800 nm via $S = 1-T-R$, with direct optical transmittance T and specular reflection R). Both, steam treatment and weathering in the climate control chamber, result in higher surface roughness in SLS glass [6], [44], [45]. For the IOX glass, this effect is much weaker, assumedly as a result of improved resistance to surface degradation following potassium-for-sodium exchange and the higher solubility of potassium carbonates in water. SEM micrographs of the different surface states are shown by way of example in Figs. 2C-F, confirming this interpretation. On the steam-treated SLS glass (Fig. 2C), pronounced formation of µm-scale residue features is observed, whereas the steam treated IOX glass does not exhibit such surface degradation (Fig. 2E). Similar observations are made on the weathered glass surfaces ("CC" samples, Figs. 2D-F). Overall, these results indicate how chemical strengthening of SLS glass improves the chemical durability of its surface in terms of the formation of optically scattering residues. This is an important feature, as it suggests a more sensible use of water/steam treatment on these glasses for altering surface mechanical properties without degrading surface appearance.
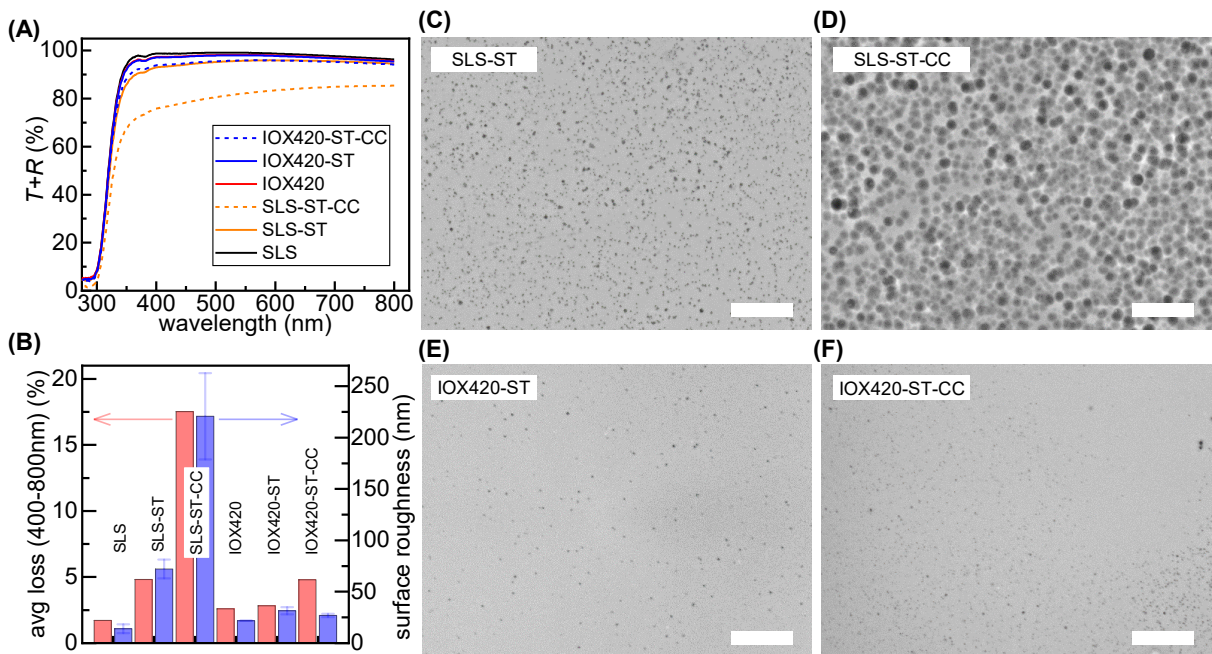
Figure 2. *(A) Sum of direct optical transmission (T) and specular reflection (R) of pristine SLS, IOX glasses and materials after steam treatment ("ST") and subsequent long-term weathering ("ST-CC"). (B) Average optical loss in the wavelength range between 400 and 800 nm (red bars) and surface roughness (RMS, blue bars). (C-F) SEM micrographs of glass surfaces of SLS (C,D) and IOX glass (E,F) after steam treatment (C,D) and after subsequent weathering for 1030 h at 80 °C and 80 %r.H. The scale bars are 10 µm.*

Surface hardness

The impact of steam treatment on the indentation deformation and the scratch hardness of SLS and IOX glasses is presented in Figure 3, revealing the expected increase of both indentation hardness, H (Fig. 3A) and surface Young's modulus E (Fig. 3B) upon ion-exchange [14], [21], [44]–[47].

While steam treatment does not have any notable effect on the bulk indentation response at a depth exceeding 500 nm, it leads to a reduction of hardness and stiffness in the upper surface to a depth of few hundred nanometers [48], [49]. In all cases, the affected depth is much lower than the IOX DOL, what might be the reason for the unaffected stress profiles (Fig. 1A). The softening effect is qualitatively strongest for the steam-treated SLS glass, but

pronounced corrosion (see **Fig. 2C**) lead to an inhomogeneous indentation response in this case. Much more homogeneous depth profiles are obtained for the IOX samples (**Figs. 3A-B**).
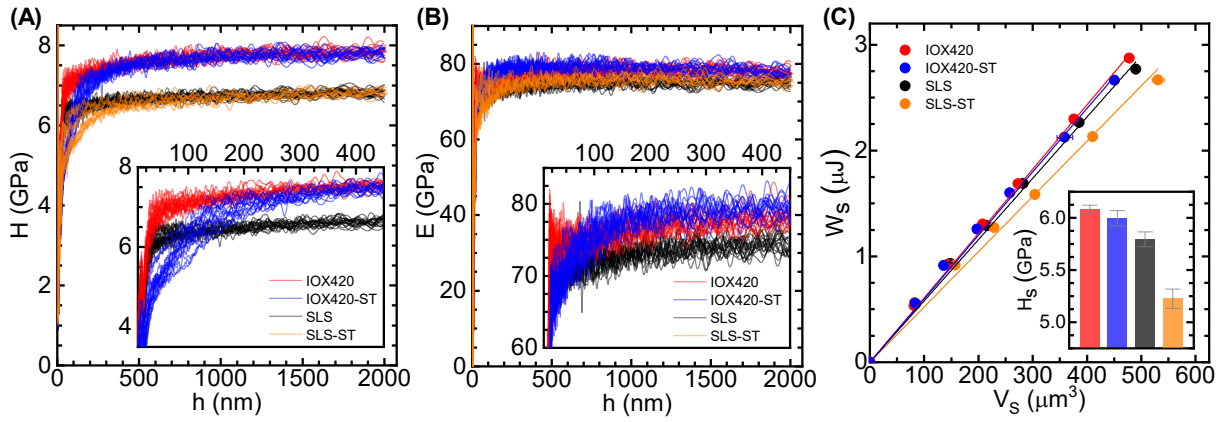
Figure 3. *Indentation depth-profiles of (A) hardness H and (B) Young's Modulus E of pristine SLS, IOX glasses and the corresponding materials after steam treatment ("ST"). The insets in (A-B) highlight the surface regions to a depth of 450 nm (excluding the SLS-ST sample because of high scattering, assumedly resulting from the surface corrosion seen in Fig. 2C). (C) Work of deformation, W_s, over scratched volume, V_s, and corresponding linear fits. The inset in (C) shows the corresponding scratch hardness values, H_s determined from the slopes of the linear regression curves according to reference [38].*

In addition to indentation hardness, the scratch hardness was determined using a constant load scratch test with a sharp Berkovich tip [36], [50]. The work of deformation W_S obtained as a function of scratched volume V_S is shown in Fig. 3C. Very similar dependencies were found in this experiment for all glasses except for SLS-ST, which exhibited a significant decrease in scratch hardness $H_S = dW_S (dV_S)^{-1}$ (Fig. 3C, $H_S^{SLS} = 5.79 \pm 0.07$ GPa, $H_S^{SLS-ST} = 5.22 \pm 0.09$ GPa). As with the softening in normal indentation, this decrease is attributed to surface corrosion, reducing the glass' resistance against lateral plowing (Fig. 3C).[51] Aside from this observation, the effect of steam treatment on sharp scratching of IOX glasses is within the accuracy of data acquisition ($H_S^{IOX420} = 6.08 \pm 0.04$ GPa, $H_S^{IOX420-ST} = 6.00 \pm 0.07$ GPa). The minor decrease in H_S following steam treatment probably reflects the softer surface layer seen in normal indentation (Fig. 3A; in the normal load range of $P_N = 30 - 150$ mN, the residual scratch depth was ~ 180 – 450 nm, therefore, the observed scratch hardness is partially affected by the surface softness).

Scratching behavior and abrasion

The observed surface softening by steam treatment had substantial effects on the glass' defect susceptibility and damage infliction behavior during scratching. In order to resolve variations in ductile yielding and the statistics of microcracking and brittle abrasion, scratching was conducted at a low apex load using a sphero-conical stylus [21], [37]. Microscopic images of typical scratch grooves generated in this way are shown in Figure 4, together with *in-situ* data of the displacement into the surface h and the build-up of lateral force F_L acting on the tip as functions of the gradually increasing normal load applied on the indenter (and the length of the scratch distance created at a constant sliding speed of 50 μm s^{-1}). The most prominent features in these profiles are the onsets of microcracking and of abrasive wear, visible in local bursts in the h data and a sudden increase in the F_L plot, respectively (in addition, both events qualitatively recur in the post mortem scratch profiles, which also enable to distinguish between microcracks formed during scratching or after unloading, that is, after the stylus has passed a certain region of the sample [21]).
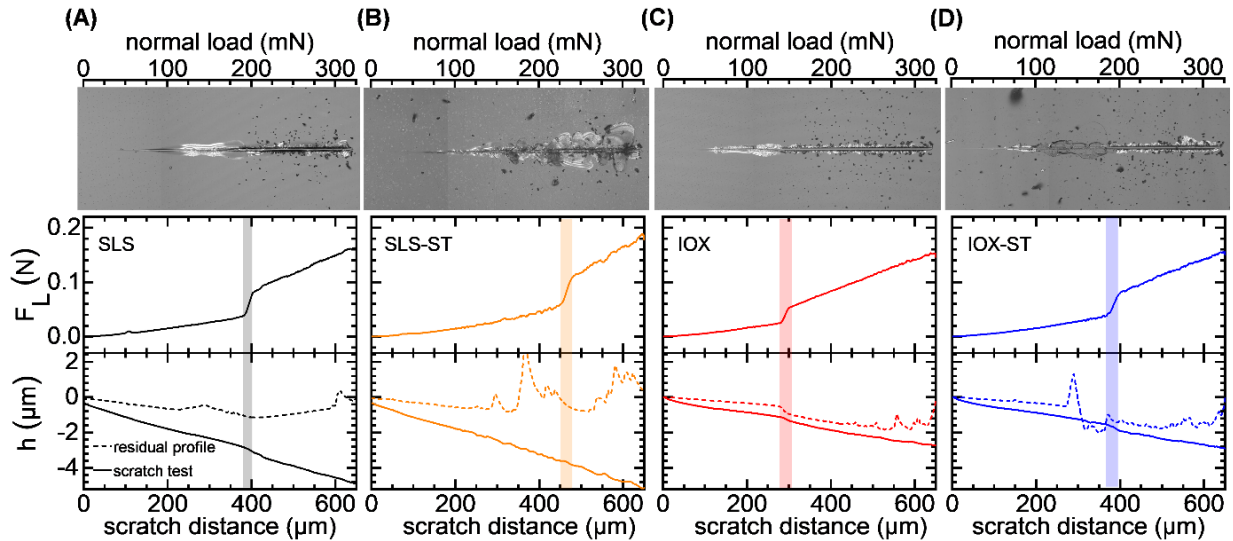
Figure 4. *Examples of ramp-load scratch tests showing the build-up of lateral force F_L acting on the tip and the depth h of the scratch groove during scratching using a sphero-conical diamond stylus with a nominal radius of 5.1 μm (solid lines; dashed lines depict the residual depth profiles recorder after unloading by re-tracing the stylus at a constant normal load of 50 μN). Top: optical micrographs of the residual scratch grooves. (A) Pristine SLS; (B) steam-treated SLS ("ST"); (C) ion-exchanged, and (D) ion-exchanged and steam-treated glass.*

As seen in Figure 4, the onset of microabrasion is strongly affected by the surface state. IOX leads to a shift to lower normal loads (Fig. 4B), in accordance with previous observations [21]: ion stuffing reduces the surface resistance to brittle abrasion. However, subsequent steam treatment compensates this effect (Fig. 4D). A statistical analysis of the load thresholds for microcracking and abrasive wear is shown in Figure 5, using data from up to 25 individual scratch tests per specimen.
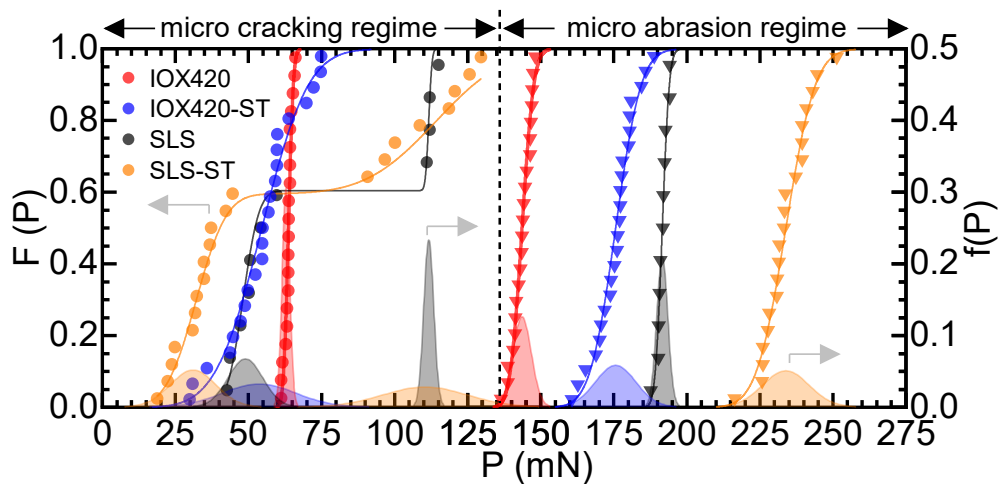
Figure 5. *Statistical analysis of the load thresholds for microcracking and microabrasion in pristine SLS, IOX glasses and the corresponding materials after steam treatment ("ST"). Data represent the cumulative probability F(P) (scatter plots) and probability density f(P) (shaded areas) of the normal load P at the onset of microcracking and microabrasion. A bimodal distribution of the onset of microcracking originates from the presence of multiple defect modes, in particular, random preexisting defects which are suppressed by the compressive stress profile in the IOX glasses [21].*

The two SLS glasses (SLS and SLS-ST) exhibit a bimodal distribution of the load threshold for microcracking, caused by random, pre-existing surface defects [21]. The steam-treated SLS-

ST has the highest propensity for microcracking at the low-load failure mode, which we attribute to defect growth by surface corrosion (Fig. 2C). The low-load failure mode is completely suppressed in the IOX glasses, which have a mono-modal failure distribution for microcracking. In all glasses, stream treatment causes a minor shift of the microcracking onset (high-load failure modes) to slightly lower normal load. In addition, there is a broadening of the microcracking probability density distribution upon steam treatment. For the IOX glass, the former is attributed to a release of top-layer surface stress (counteracting microcracking), while the latter indicates inhomogeneous defect growth during steam treatment.

More importantly, the onset of microabrasion is strongly shifted to higher normal loads following steam treatment. Such a strong effect might be somewhat expected for the steam-treated SLS glass, where treatment caused surface corrosion (Figs. 2C, 3A) resulting in enhanced plastic deformation during lateral loading (also visible in the reduced scratch hardness, see Fig. 3C). It is more interesting for the steam-treated IOX glass, in which severe autoclave corrosion was suppressed by IOX stuffing.

The abrasive wear resistance is more strongly affected by the steam treatment than the scratch hardness (Fig. 3C). This is initially somewhat unexpected given the larger penetration depth of the sphero-conical indenter tip at the onset of microabrasion (Fig. 4D) in comparison to the displacement range considered for the evaluation of scratch hardness. However, abrasive scratching is dominated by chipping events near the apex of the sliding indenter tip. The glass surface is the most likely location to initiate crack growth. It is therefore not surprising that the state of the upper surface layer defines the threshold for microabrasion disproportionately.

4. Conclusion

While the detailed mechanism of surface softening in steam-treated IOX glass remains unresolved, it is clearly associated with stress relaxation [29], [52], proton exchange reactions leading to reduced stuffing levels[48], [49], [53] and indeed hydration of the top surface [45], [51], [54], [55]. As a result, autoclave steam-treatment presents a way to partially compensate the enhanced surface brittleness accompanying IOX. This causes a notable shift in the load threshold for microabrasion to more abrasion-resistant glasses. Within the range of the current processing parameters, the softening effect is constrained to a surface layer of less than 500 nm in thickness, therefore, the overall compressive stress profile is not affected.

Data Availability Statement

The data that support the findings of this study are available from the corresponding author upon reasonable request.

Underlying and related material

Correspondence and requests should be addressed to corresponding author Lothar Wondraczek.

Author Contributions

G. Sani: Investigation, Formal analysis, Writing - Original Draft **R. Sajzew:** Methodology, Investigation, Formal analysis, Visualization, Writing - Original Draft **R. Limbach:** Methodology, Writing - Original Draft, **S. Sawamura:** Writing - Review & Editing **A. Koike:** Writing - Review & Editing **L. Wondraczek:** Conceptualization, Methodology, Writing - Review & Editing, Project administration, Funding acquisition, Resources.

Competing interests

Funding

Acknowledgments

References

[1] S. M. Wiederhorn and D. R. Clarke, "Architectural Glass," *Annu Rev Mater Res*, vol. 52, pp. 561–592, 2022, doi: https://doi.org/10.1146/annurev-matsci-101321-014417.

[2] K. Klaiman, D. L. Ortega, and C. Garnache, "Consumer preferences and demand for packaging material and recyclability," *Resour Conserv Recycl*, vol. 115, pp. 1–8, Dec. 2016, doi: https://doi.org/10.1016/J.RESCONREC.2016.08.021.

[3] J. Zimmer, "Invited paper: Novel thin glass for 3D shaped electronics display covers," *49th Annual SID Symposium, Seminar, and Exhibition 2011, Display Week 2011*, vol. 2, pp. 833–836, 2011, doi: https://doi.org/10.1889/1.3621462.

[4] S. Addanki, I. S. Amiri, and P. Yupapin, "Review of optical fibers-introduction and applications in fiber lasers," *Results Phys*, vol. 10, no. July, pp. 743–750, 2018, doi: https://doi.org/10.1016/j.rinp.2018.07.028.

[5] S. Chen, M. Zang, D. Wang, S. Yoshimura, and T. Yamada, "Numerical analysis of impact failure of automotive laminated glass: A review," *Compos B Eng*, vol. 122, pp. 47–60, 2017, doi: https://doi.org/10.1016/j.compositesb.2017.04.007.

[6] M. Ciccotti, "Stress-corrosion mechanisms in silicate glasses," *J Phys D Appl Phys*, vol. 42, no. 21, p. 214006, 2009, doi: https://doi.org/10.1088/0022-3727/42/21/214006.

[7] A. K. Varshneya, "Stronger glass products: Lessons learned and yet to be learned," *Int J Appl Glass Sci*, vol. 9, no. 2, pp. 140–155, Apr. 2018, doi: https://doi.org/10.1111/ijag.12341.

[8] R. E. Mould, "The Strength of Inorganic Glasses," in *Fracture of Metals, Polymers, and Glasses*, Boston, MA: Springer US, 1967, pp. 119–149. doi: https://doi.org/10.1007/978-1-4684-3153-7_7.

[9] L. Wondraczek *et al.*, "Towards ultrastrong glasses," *Advanced Materials*, vol. 23, no. 39, pp. 4578–4586, Oct. 2011, doi: https://doi.org/10.1002/adma.201102795.

[10] T. Rouxel and S. Yoshida, "The fracture toughness of inorganic glasses," *Journal of the American Ceramic Society*, vol. 100, no. 10, pp. 4374–4396, Oct. 2017, doi: https://doi.org/10.1111/jace.15108.

[11] J. Sehgal and S. Ito, "A new low-brittleness glass in the soda-lime-silica glass family," *Journal of the American Ceramic Society*, vol. 81, no. 9, pp. 2485–2488, Jan. 2005, doi: https://doi.org/10.1111/j.1151-2916.1998.tb02649.x.

[12] K. S. R. Karlsson and L. Wondraczek, "Strengthening of Oxide Glasses," *Encyclopedia of Glass Science, Technology, History, and Culture*, pp. 391–404, Feb. 2021, doi: https://doi.org/10.1002/9781118801017.CH3.12.

[13]   R. Sajzew and L. Wondraczek, "Thermal strengthening of low-expansion glasses and thin-walled glass products by ultra-fast heat extraction," *Journal of the American Ceramic Society*, vol. 104, no. 7, pp. 3187–3197, 2021, doi: https://doi.org/10.1111/jace.17759.

[14]   R. Gy, "Ion exchange for glass strengthening," *Mater Sci Eng B Solid State Mater Adv Technol*, vol. 149, no. 2, pp. 159–165, 2008, doi: https://doi.org/10.1016/j.mseb.2007.11.029.

[15]   A. K. Varshneya, "Chemical Strengthening of Glass: Lessons Learned and Yet To Be Learned," *Int J Appl Glass Sci*, vol. 1, no. 2, pp. 131–142, 2010, doi: https://doi.org/10.1111/j.2041-1294.2010.00010.x.

[16]   L. Wondraczek, E. Bouchbinder, A. Ehrlicher, J. C. Mauro, R. Sajzew, and M. M. Smedskjaer, "Advancing the Mechanical Performance of Glasses: Perspectives and Challenges," *Advanced Materials*, vol. 34, no. 14, p. 2109029, Apr. 2022, doi: https://doi.org/10.1002/ADMA.202109029.

[17]   E. Guadagnino, M. Guglielmi, and F. Nicoletti, "Glass: The best material for pharmaceutical packaging," *Int J Appl Glass Sci*, vol. 13, no. 3, pp. 281–291, Jul. 2022, doi: https://doi.org/10.1111/IJAG.16559.

[18]   B. P. V Heiz *et al.*, "Ultrathin Fluidic Laminates for Large-Area Façade Integration and Smart Windows," *Advanced Science*, vol. 4, no. 3, p. 1600362, Mar. 2017, doi: https://doi.org/10.1002/ADVS.201600362.

[19]   S. Karlsson, S. Ali, R. Limbach, M. Strand, and L. Wondraczek, "Alkali salt vapour deposition and in-line ion exchange on flat glass surfaces," *Glass Technology: European Journal of Glass Science and Technology Part A*, vol. 56, no. 6, pp. 203–213, Dec. 2015, doi: 1 https://doi.org/0.13036/1753-3546.56.6.203.

[20]   S. Karlsson, L. Wondraczek, S. Ali, and B. Jonson, "Trends in effective diffusion coefficients for ion-exchange strengthening of soda-lime-silicate glasses," *Front Mater*, vol. 4, p. 13, Apr. 2017, doi: https://doi.org/10.3389/fmats.2017.00013.

[21]   G. Sani, R. Limbach, J. Dellith, İ. Sökmen, and L. Wondraczek, "Surface damage resistance and yielding of chemically strengthened silicate glasses: From normal indentation to scratch loading," *Journal of the American Ceramic Society*, vol. 104, no. 7, pp. 3167–3186, 2021, doi: https://doi.org/10.1111/jace.17758.

[22]   C. Ragoen, M. A. T. Marple, S. Sen, T. Lambricht, and S. Godet, "Structural modifications induced by Na+/K+ ion exchange in silicate glasses: A multinuclear NMR spectroscopic study," *J Non Cryst Solids*, vol. 474, no. August, pp. 9–15, 2017, doi: https://doi.org/10.1016/j.jnoncrysol.2017.08.006.

[23]   C. Ragoen, S. Sen, T. Lambricht, and S. Godet, "Effect of Al2O3 content on the mechanical and interdiffusional properties of ion-exchanged Na-aluminosilicate glasses," *J Non Cryst Solids*, vol. 458, pp. 129–136, 2017, doi: https://doi.org/10.1016/j.jnoncrysol.2016.12.019.

[24]   S. Karlsson *et al.*, "Mechanical, thermal, and structural investigations of chemically strengthened Na2O–CaO–Al2O3–SiO2 glasses," *Front Mater*, vol. 9, no. October, pp. 1–19, 2022, doi: https://doi.org/10.3389/fmats.2022.953759.

[25]   C. Calahoo, J. W. Zwanziger, and I. S. Butler, "Mechanical-Structural Investigation of Ion-Exchanged Lithium Silicate Glass using Micro-Raman Spectroscopy," *Journal of Physical Chemistry C*, vol. 120, no. 13, pp. 7213–7232, 2016, doi: https://doi.org/10.1021/acs.jpcc.6b01720.

[26]   F. Bengtsson, I. B. Pehlivan, L. Österlund, and S. Karlsson, "Alkali ion diffusion and structure of chemically strengthened TiO2 doped soda-lime silicate glass," *J Non Cryst Solids*, vol. 586, no. March, 2022, doi: https://doi.org/10.1016/j.jnoncrysol.2022.121564.

[27]   A. K. Varshneya, G. Macrelli, S. Yoshida, S. H. Kim, A. L. Ogrinc, and J. C. Mauro, "Indentation and abrasion in glass products: Lessons learned and yet to be learned," *Int J Appl Glass Sci*, no. October 2021, pp. 1–30, 2021, doi: https://doi.org/10.1111/ijag.16549.

[28]   S. Karlsson, B. Jonson, and C. Stålhandske, "The technology of chemical glass strengthening - A review," *Glass Technology: European Journal of Glass Science and Technology Part A*, vol. 51, no. 2, pp. 41–54, 2010.

[29] P. J. Lezzi, Q. R. Xiao, M. Tomozawa, T. A. Blanchet, and C. R. Kurkjian, "Strength increase of silica glass fibers by surface stress relaxation: A new mechanical strengthening method," *J Non Cryst Solids*, vol. 379, pp. 95–106, Nov. 2013, doi: https://doi.org/10.1016/J.JNONCRYSOL.2013.07.033.

[30] T. M. Gross *et al.*, "Glass with hydration-induced compressive stress profiles," *Journal of the American Ceramic Society*, vol. 105, no. 4, pp. 2527–2535, Apr. 2022, doi: https://doi.org/10.1111/JACE.18191.

[31] T. M. Gross and J. Wu, "Design of mechanically advantaged glasses with hydration-induced stress profiles," *Int J Appl Glass Sci*, vol. 14, no. 1, pp. 18–26, Jan. 2023, doi: https://doi.org/10.1111/IJAG.16597.

[32] P. Kiefer *et al.*, "Density, elastic constants and indentation hardness of hydrous soda-lime-silica glasses," *J Non Cryst Solids*, vol. 521, p. 119480, Oct. 2019, doi: https://doi.org/10.1016/J.JNONCRYSOL.2019.119480.

[33] T. Waurischk *et al.*, "Crack Growth in Hydrous Soda-Lime Silicate Glass," *Front Mater*, vol. 7, p. 66, Mar. 2020, doi: 10.3389/fmats.2020.00066.

[34] T. Kishii, "Surface stress meters utilising the optical waveguide effect of chemically tempered glasses," *Opt Lasers Eng*, vol. 4, no. 1, pp. 25–38, 1983, doi: https://doi.org/10.1016/0143-8166(83)90004-0.

[35] S. Reiß, S. Krischok, and E. Rädlein, "Comparative study of weather induced corrosion mechanisms of toughened and normal float glasses," *Glass Technology: European Journal of Glass Science and Technology Part A*, vol. 60, no. 2, pp. 33–44, 2019, doi: https://doi.org/10.13036/17533546.60.2.020.

[36] S. Sawamura, R. Limbach, H. Behrens, and L. Wondraczek, "Lateral deformation and defect resistance of compacted silica glass: Quantification of the scratching hardness of brittle glasses," *J Non Cryst Solids*, vol. 481, pp. 503–511, 2018, doi: https://doi.org/10.1016/j.jnoncrysol.2017.11.035.

[37] S. Sawamura, R. Limbach, S. Wilhelmy, A. Koike, and L. Wondraczek, "Scratch-induced yielding and ductile fracture in silicate glasses probed by nanoindentation," *Journal of the American Ceramic Society*, vol. 102, no. 12, pp. 7299–7311, Dec. 2019, doi: https://doi.org/10.1111/jace.16679.

[38] S. Sawamura and L. Wondraczek, "Scratch hardness of glass," *Phys Rev Mater*, vol. 2, no. 9, p. 92601, 2018, doi: https://doi.org/10.1103/PhysRevMaterials.2.092601.

[39] M. E. Nordberg, E. L. Mochel, H. M. Garfinkel, and J. S. Olcott, "Strengthening by Ion Exchange," *Journal of the American Ceramic Society*, vol. 47, no. 5, pp. 215–219, 1964, doi: https://doi.org/10.1111/j.1151-2916.1964.tb14399.x.

[40] R. F. Bartholomew, B. L. Butler, H. L. Hoover, and C. K. Wu, "Infrared Spectra of a Water-Containing Glass," *Journal of the American Ceramic Society*, vol. 63, no. 9–10, pp. 481–485, Sep. 1980, doi: https://doi.org/10.1111/J.1151-2916.1980.TB10748.X.

[41] A. Stuke, H. Behrens, B. C. Schmidt, and R. Dupree, "H2O speciation in float glass and soda lime silica glass," *Chem Geol*, vol. 229, no. 1–3, pp. 64–77, 2006, doi: https://doi.org/10.1016/j.chemgeo.2006.01.012.

[42] C.-K. Wu, "Nature of Incorporated Water in Hydrated Silicate Glasses," *Journal of the American Ceramic Society*, vol. 63, no. 7–8, pp. 453–457, Jul. 1980, doi: https://doi.org/10.1111/j.1151-2916.1980.tb10211.x.

[43] R. H. Doremus, "Exchange and diffusion of ions in glass," *Journal of Physical Chemistry*, vol. 68, no. 8, pp. 2212–2218, 1964, doi: https://doi.org/10.1021/j100790a031.

[44] Y. A. Gösterişlioğlu, A. E. Ersundu, M. Çelikbilek Ersundu, and Sökmen, "Investigation the effect of weathering on chemically strengthened flat glasses," *J Non Cryst Solids*, vol. 544, no. June, 2020, doi: https://doi.org/10.1016/j.jnoncrysol.2020.120192.

[45] X. Li, L. Jiang, J. Liu, M. Wang, J. Li, and Y. Yan, "Insight into the interaction between water and ion-exchanged aluminosilicate glass by nanoindentation," *Materials*, vol. 14, no. 11, pp. 1–12, 2021, doi: https://doi.org/10.3390/ma14112959.

[46] R. Tandon and D. J. Green, "Indentation Behavior of Ion-Exchanged Glasses," *Journal of the American Ceramic Society*, vol. 73, no. 4, pp. 970–977, 1990, doi: https://doi.org/10.1111/j.1151-2916.1990.tb05145.x.

[47] A. Talimian and V. M. Sglavo, "Can annealing improve the chemical strengthening of thin borosilicate glass?," *J Non Cryst Solids*, vol. 465, pp. 1–7, 2017, doi: https://doi.org/10.1016/j.jnoncrysol.2017.03.038.

[48] W. A. Lanford, K. Davis, P. Lamarche, T. Laursen, R. Groleau, and R. H. Doremus, "Hydration of soda-lime glass," *J Non Cryst Solids*, vol. 33, no. 2, pp. 249–266, Jun. 1979, doi: https://doi.org/10.1016/0022-3093(79)90053-X.

[49] T. Fett, J. P. Guin, and S. M. Wiederhorn, "Stresses in ion-exchange layers of soda-lime-silicate glass," *Fatigue Fract Eng Mater Struct*, vol. 28, no. 6, pp. 507–514, 2005, doi: https://doi.org/10.1111/j.1460-2695.2005.00888.x.

[50] G. N. B. M. B. M. de Macedo, S. Sawamura, and L. Wondraczek, "Lateral hardness and the scratch resistance of glasses in the Na2O-CaO-SiO2 system," *J Non Cryst Solids*, vol. 492, pp. 94–101, 2018, doi: https://doi.org/10.1016/j.jnoncrysol.2018.04.022.

[51] D. R. Tadjiev and R. J. Hand, "Surface hydration and nanoindentation of silicate glasses," *J Non Cryst Solids*, vol. 356, no. 2, pp. 102–108, 2010, doi: https://doi.org/10.1016/j.jnoncrysol.2009.10.005.

[52] S. S. Kistler, "Stresses in Glass Produced by Nonuniform Exchange of Monovalent Ions," *Journal of the American Ceramic Society*, vol. 45, no. 2, pp. 59–68, 1962, doi: https://doi.org/10.1111/j.1151-2916.1962.tb11081.x.

[53] A. Michalske and B. C. Bunker, *Effect of Surface Stress on Stress Corrosion of Silicate Glass*, no. V. International Congress on Fracture (ICF), 1989. doi: https://doi.org/10.1016/b978-0-08-034341-9.50256-4.

[54] M. Takata, M. Tomozawa, and E. B. Watson, "Effect of Water Content on Mechanical Properties of Na2O-SiO2 Glasses," *Journal of the American Ceramic Society*, vol. 65, no. 9, pp. c156–c157, Sep. 1982, doi: https://doi.org/10.1111/j.1151-2916.1982.tb10525.x.

[55] B. C. Bunker, G. W. Arnold, E. K. Beauchamp, and D. E. Day, "Mechanisms for alkali leaching in mized-NaK silicate glasses," *J Non Cryst Solids*, vol. 58, no. 2–3, pp. 295–322, 1983, doi: https://doi.org/10.1016/0022-3093(83)90031-5.